OPTICAL AND PHOTOLUMINESCENCE CHARACTERISTICS OF POLYCRYSTALLINE ZINC OXIDE THIN FILMS

D.I. RUSU[a*], I. EVTODIEV[b], I. CARAMAN[a], G. RUSU[c]
[a] *„V. Alecsandri" University of Bacau, 157 Calea Marasesti, 600115 Bacau, Romania*
[b] *Moldova State University, 60 A. Mateevici Str., Chisinau, MD-2009, Republic of Moldova*
[c] *Faculty of Physics, „Al. I. Cuza" University, 11 Carol I Blvd., 700506 Iasi, Romania*

Zinc oxide (ZnO) thin films were prepared by thermal oxidation in open atmosphere of vacuum evaporated zinc metallic films. The investigations of film structure, performed by X-ray diffraction technique, showed that ZnO films are polycrystalline and have a würtzite (hexagonal) structure with film crystallites preferentially oriented with (002) planes parallel to the substrate surface. Some values of structural parameters (lattice constants of würtzite cell, crystallite size, Zn-O bond length) of the ZnO films were determined. The transsmision and absorption spectra were studied for incident photon energies ranged between 1.50 eV and 4.50 eV. The optical energy bandgap, calculated from the absorption spectra, is ranged from 3.36 eV to 3.45 eV. Photoluminescence (PL) spectra at temperatures 293 K and 78 K have been analysed. The PL is dominated by the emission at 3.338 eV. Temperature dependence of the intensity of the main peaks has been discussed.

(Received June 3, 2014; Accepted July 12, 2014)

Keywords: Zinc oxide, Thin films, Thermal oxidation, Photoluminescence

1. Introduction

Transparent conductive oxides (TCOs) constitute an important class of semiconducting materials that combine their high optical transmission coefficients in the visible and near infrared spectral ranges with a high electrical conductivity at room temperature [1-5].

Zinc oxide (ZnO) is a representative compound of this class which has attracted considerable attention owing to its large number of applications such as transparent field-effect transistors, energy-efficient windows, transparent electrodes, flat panel displays, solar cells, ozone detectors, etc. [6-10]. These important applications are based on the intersting optical and electronic transport properties of ZnO (high transparency in the visible spectral range of the solar spectrum, wide direct energy bandgap of 3.37 eV, low electrical resistivity at room temperature, high thermal and chemical stability, etc.) which are very suitable for various new applications in modern solid-state device technologies: nanoscale transparent electronics, sensor tehnology, optoelectronics, etc. [1,3,8,9]. Several different techniques have been successfully employed to prepare transparent conductive ZnO thin films, such as magnetron sputtering, spray pyrolysis, chemical vapor deposition, sol-gel (spin coating), pulsed laser deposition, molecular beam epitaxy, etc. [11-19].

Many of the semiconducting properties of ZnO thin films strongly depend on their structural characteristics and non-stoichiometric composition, which in turn depend on the used preparation method and deposition conditions.

---

[*] Corresponding author: d_i_rusu@yahoo.com.

However, there are relatively few investigations with respect to the structural, electronic transport and optical properties of ZnO thin films prepared by thermal oxidation of thin zinc metallic films [5,18,20-24].

As compared to other preparation techniques, dry thermal oxidation has many advantages such as a rigorous control on the deposition parameters (and, consequently, on the film structure), zinc films can be deposited easily by many methods, large possibilities for preparation of pure and doped ZnO thin films, a low-cost of semiconducting devices, etc.

Previously, we studied the dependence of structural and optical properties of zinc oxide thin films prepared by thermal oxidation of zinc metallic films in different conditions [5,21,22,24]. Some correlations between preparation conditions and structural characteristics of ZnO thin films have been established.

On the other hand, due to both theoretical interest and technological importance, the photoluminescence properties of ZnO thin films have been intensively and sistematically studied in the last years paying special attention to the low temperature range [6,9,12,25-27].

ZnO is also a potential candidate for the active films in some important modern devices (laser diodes, light-emitting diodes, etc.) due to their large exciton binding energy (about 60 meV), which gives assurance of an efficient excitonic emission up to room temperature [1,6,10,27].

In the present paper we extended investigations on the ZnO thin films prepared by thermal oxidation of vacuum evaporated Zn films by studying transmission and absorption spectra (in wavelength range from 300 nm to 1600 nm) and at temperatures of 78 K and 293 K. The photoluminiscence properties of respective films in mentioned wavelength range are also investigated.

2. Experimental

Zinc thin films were deposited by thermal evaporation under vacuum onto optically flat glass (Corning 1737) and amorphous SiO_2 substrates at room temperature (T=293 K). The experimental arrangement used for preparation of zinc metallic thin films was similar to one previously reported [21,22,24,28].

The high purity (99.99 wt%) zinc powder (Aldrich) was used as starting material. The source (evaporator) to substrate distance was maintained to be 9 cm and deposition rate was about 10 Å/s in all cases.

The thickness of Zn and ZnO films was determined using Fizeau's method for fringes of equal thickness [30] at reflection of monochromatic light (λ=550 nm). An interferential microscope MII-4 (LOMO, St. Petersburg) was used for measurements. Thickness of studied ZnO thin films ranged between 140 nm and 1600 nm.

The crystalline structure of the films was analyzed by X-ray diffraction (XRD) technique using a DRON-3 diffractometer (with CuK_α radiation, λ=1.5418 Å). The X-ray patterns were recorded in the 2θ range from 20° to 80°.

The thermal oxidation procedure of zinc thin films consisted of following successive technological steps: (i) a heating, in open atmosphere, (relative humidity was about 60%), in the temperature range from 300 K to T_{ox} (where T_{ox} denotes oxidation temperature), with a temperature rate of about 6 K/min; (ii) an annealing for a certain oxidation time, t_{ox} (t_{ox}=30-120 min) at a determined oxidation temperature (T_{ox}=500-870 K); (iii) a cooling from oxidation temperature to room temperature, with a temperature rate of about 10 K/min. We experimentally established that these preparation conditions permit to prepare ZnO thin films having a homogeneous structure, good crystalline quality, stable stoichiometry and very good adhesion to the substrate surface [22].

The thin film preparation set-up and used measuring technique have in detail described elsewhere [21,22,24].

After oxidation, the metallic films become transparent in visible spectral range.

The reflection and transmission spectra, in vicinity of fundamental absorption band edge (corrected for the effect of the glass substrate [6,17,29,30]), in the spectral range from 300 nm to

1600 nm, were recorded at 78 K and 293 K using a Steag ETA Optik computer controlled spectrometer and a Specord UV-VIS-M.40 (C. Zeiss, Jena) spectrophotometer.

The absorption coefficient, α, at temperatures 78 K and 293 K, was calculated from the expression [29-31]

$$\alpha = \frac{1}{d}\ln\left[\frac{\left[(1-R)^4+4+2R^2\right]^{1/2}+(1-R)^2}{2T}\right] \tag{1}$$

where d is the film thickness and R and T are reflection coefficient and transmission coefficient, respectively.

This relationship is valid for normal incidence and in absence of interference effects.

Photoluminescence (PL) was measured at room temperature, using a setup described in [32,33]. For studied films the following preparation conditions were used: oxidation temperature, T_{ox}=750 K; oxidation time was, t_{ox}=60 min; film thickness, d=140 nm. The excitation of photoluminescence was performed by using as excitation source the monochromatic radiation (λ=337.4 nm) from an N_2 laser emitting pulses at a frequency up to 82 Hz.

For measurements at 78 K, the samples under study were placed upside down in an N_2 vapor atmosphere, into a cryostat with quartz windows [32].

The PL spectra at temperature 78 K were recorded by a monochromator MDR-2 with a diffraction grating (1200 mm^{-1}) and as detector was a photomultiplier having cathodes of $(Na_2K)Sb:Cs$ with energetic resolution of about 0.5 meV [32].

3. Results and discussion

3.1 Microstructural characteristics

More detailed investigations on the correlation between microstructural characteristics and preparation conditions of ZnO thin films obtained by oxidation of zinc metallic films are reported in our previous paper. [22]

For ZnO thin films studied in present paper the following values of main preparation parameters were used: zinc films were deposited, by vacuum thermal evaporation, onto glass substrates (the deposition conditions are indcated in precedent section); oxidation temperature was T_{ox}= 700 K; oxidation time, t_{ox}= 30 min; the thickness of ZnO films was about 270 nm.

After preparation, thin film ZnO samples were submitted to a heat treatment, consisting of several heating/cooling cycles (usually, 2-3 cycles) within a temperature range ΔT=300-550 K. Consequently, the films with stable solide-state structure have been obtained and the temperature dependence of the electrical conductivity becomes reversible. After this heat treatment, the preferentially orientation of the crystallites (texture coefficients) are unchanged.

A typical XRD pattern is presented in Fig.1 for a ZnO thin film (with thickness d=270 nm) prepared by described method. Different peaks were indexed and the values of the interplanar spacing, d_{hkl}, were determined and compared with a standard values for ZnO polycrystalline powder (ASTM Data) [34,35].

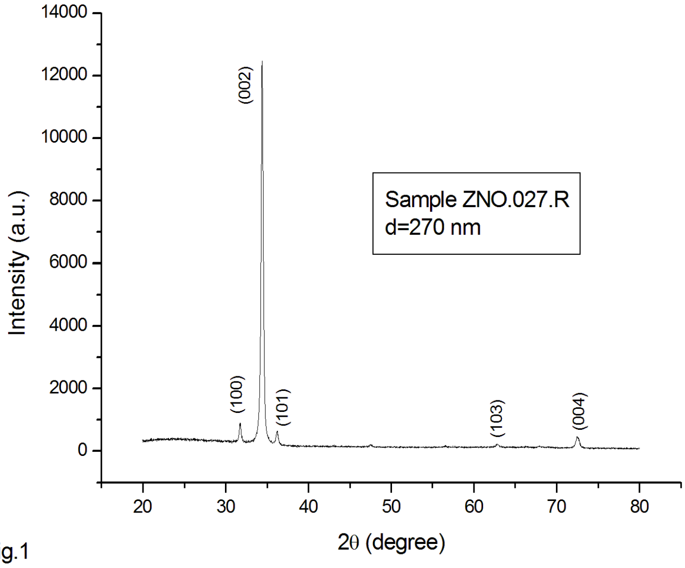

Fig.1

Fig. 1. XRD pattern of ZnO thin film sample ZNO.027.R (d=270 nm, T_{ox}=700 K, t_{ox}=30 min.).

The XRD pattern analysis showed that ZnO films are polycrystalline and have a single phase with hexagonal (würtzite) structure, generally, with three intense peaks located at 31.72°, 34.38° and 36.25°, associated with chrystallographic planes (100), (002) and (101), respectively. The other secondary weak peaks of ZnO würtzite structure ((103), (004), etc.) were also evidenced.

The presence of other phases in Zn-O system as well as of unoxidized Zn microcrystallites, was not identified for films with thickness d<1350 nm [22,24,28].

The lattice parameters of ZnO würtzite (hexagonal) structure, a and c, were calculated using well-known analytic method [21,22,34-36]. Some structural characteristics of one ZnO thin films are presented in Table 1. The obtained values of a and c are in agreement with those of ZnO, given in JCPDS data cards [34] (standard values for polycrystalline powder are: a_0=3.249 Å, c_0=5.206 Å).

Table 1 - Values of structural parameters of the investigated ZnO thin films.

Sample	*2θ* [degree]	(hkl)	d_{hkl} (Å)	D (Å)	a (Å)	c (Å)	L (Å)
ZNO.027.R	31.72	(100)	2.819	165	3.259	-	1.913
	34.38	(002)	2.606	145	-	5.213	1.913
	36.25	(101)	2.482	185	-	-	-

θ, Bragg angle; *(hkl)*, Miller indices; d_{hkl}, interplanar spacing of (hkl) planes; D, crystallite size; *a*, *c*, lattice parameters of the hexagonal (würtzite) structure; L, Zn-O bonds.

The average crystallite size of the films, D, were estimated by means of Debye-Scherrer formula [35].

$$D = \frac{k\lambda}{\beta_{2\theta}\cos\theta} \tag{2}$$

where k denotes the Scherrer's constant, λ is the wavelength of CuK_α radiation (λ = 1.5418 Å), θ is Bragg diffraction angle and $\beta_{2\theta}$ represents the full width at half maximum intensity of the diffraction peak located at angle θ.

Supposing that Scherrer constant, k, is equal to around 0.90 (according to the widespread practice [35,36]) and that the effect of the residual macrostrain is negligible [6,35,36], the crystallite size were calculated based on obtained data (Table 1).

For as-prepared ZnO films, the crystallites are preferentially oriented with (002) planes parallel to the substrate surface.

The used oxidation conditions of Zn films permit to obtain ZnO films with stable solid-state structure and correct stoichiometry [5,21,22] for films with thickness d<1350nm. For films with greater thickness (d>1.5μm), the XRD patterns indicate some peaks corresponding to unoxidized zinc microcrystallites. For this reason, the respective films were subjected to a heat-treatment within a temperature range ΔT=300-870 K.

As is well-known that thermal oxidation results in the important surface effects: an increase of vacancy concentration at the surface; generation of unsaturated bonds at the surface and consequently, surface state density is reduced; a large number of dislocations are generated, etc. These effects (processes) strongly influence on the photoluminescence of the thin films. An important role play crystallite shape and size and also the characteristics of the crystallite boundaries.

For studied samples, the average crystallite size, determined from Debye-Scherrer formula, ranged between 14.5 nm and 18.5 nm and are higher for films with greater thickness.
The Zn-O bond length, L, can be determined from the expression [22,37]

$$L = \left[\frac{a^2}{3} + \left(\frac{1}{2} - u\right)^2 c^2\right] \tag{3}$$

for würtzite structure the parameter, *u*, is given by [22,37]

$$u = \frac{a^2}{3c^2} + 0.25 \tag{4}$$

where *a* and *c* are lattice parameters.

Some structural parameters are presented in Table 1.

The relatively small values (for ZnO single crystals, L=2.21Å [1,27]) for our samples indicate the presence of structural defects (especially oxygen vacancies).

3.2 Optical properties

3.2.1 Absorption coefficient

For study of optical properties we selected a set of samples with stable structural and optical characteristics.

The films used for the study of the absorption coefficient have been prepared by following technology: zinc films were deposited onto amorphous SiO_2 substrates; oxidation temperature, T_{ox}=825 K; oxidation time, t_{ox}= 120 min.

For the study of the optical and photoluminescence properties of ZnO thin films, the heat treated samples were used.

It is well known that the investigation of fundamental intrinsic absorption edge provides valuable information on the value of optical bandgap, E_{g0}, characteristics of interband electronic transitions from valence band to conduction band, etc.

It was shown [5,6,22,31] that a stoichiometric pure semiconducting compound has a sharp absorbtion edge at that wavelength which corresponds to the forbidden energy gap of the respective semiconductor.

The transmission coefficient lies in the range 70%-80% in the visible and near infrared domain. This high transmission coefficient is due to relatively small roughness of the film surface. The spectral dependence of absorption coefficient, α, exhibits two regions: a power law at higher photon energy and a exponential one at lower photon energies.

The energy dependences of absorption coefficient, α, near the band edge for band-to-band transitions are given by the following expressions [6,29,31,33] (Tauc's formula [6,38]):

- for allowed direct transitions,

$$\alpha \cdot h\nu = A_a (h\nu - E_g)^{1/2} \tag{5}$$

- for forbidden direct transitions,

$$\alpha \cdot h\nu = A_f (h\nu - E_g)^{3/2} \tag{6}$$

In above expressions, hν is the incident photon energy, E_g denotes the optical bandgap, and A_a and A_f are characteristic parameters, independent of photon energy, for respective transitions. [6,29,31]

In addition to fundamental (band-to-band) absorption, the semiconducting polycrystalline films may exhibit in its absorption spectra, the impurity effects (extrinsic absorption, donor-conduction band, acceptor-valence band, acceptor-donor transitions), stoichiometry deviation, point defects, crystallite boundaries, etc. For low and moderate doping ($<10^{18}$ cm^{-3}) these effects are usually small, compared to band-to-band absorption. [6,27,33,38,39]

It is important to mention that ZnO crystals are characterized by allowed direct transitions. Consequently, according to Eq (5), in vicinity of the fundamental absorption edge, $(\alpha \cdot h\nu)^2$ linearly depends on the photon energy, hν. By extrapolating the linear portions of $(\alpha \cdot h\nu)^2$ =f(hν) dependences to $(\alpha \cdot h\nu)^2 \to 0$, the energy bandgap E_g for this type of transitions is obtained. [5,22,38,39]

In pure semiconducting materials the intrinsic absorption is dominated by exciton generation which determines a line structure direct bandgap of materials at higher temperature and a more complicated expression can be deduced for the dependence α=f(hν) at lower temperatures.

Fig.2 presents typical experimental absorption spectrum for a studied ZnO thin film, at temperatures 293 K and 78 K. The dependences α=f(hν) at temperature 293 K consists of an absorption band ($\alpha_{max}=5.8\times10^5$ cm^{-1}) with maximum at 3.343 eV. By analyzing these spectra, one can state that the edge of intrinsic absorption band of studied ZnO thin film is located in the energy range from 3.3 eV to 3.5 eV. We draw attention to the good agreement of our results with those reported for bulk ZnO crystals [1,27,36].

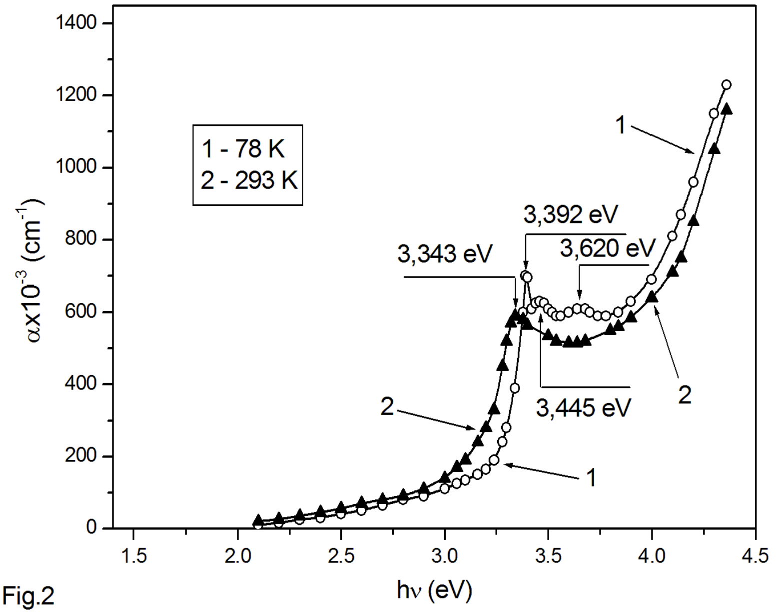

Fig.2

Fig. 2. Optical absorption edge of a typical ZnO thin films at temperatures of 293 K and 78 K.

The edge of intrinsic absorption band of ZnO single crystals is formed by excitonic bands. If the bands $h\nu_1$=3.392 eV and $h\nu_2$=3.445 eV correspond to the excitons with large radius [29,30,33].

As one can ascertain from the absorption spectra, the most complex spectrum is that recorded at 78 K. At cooling of sample at the temperature of 78 K, this maximum shifts to higher energies and splits into three bands: one at the fundamental edge with maximum at 3.392 eV and another two bands with maximums located at 3.445 eV (Fig.3) and 3.620 eV.

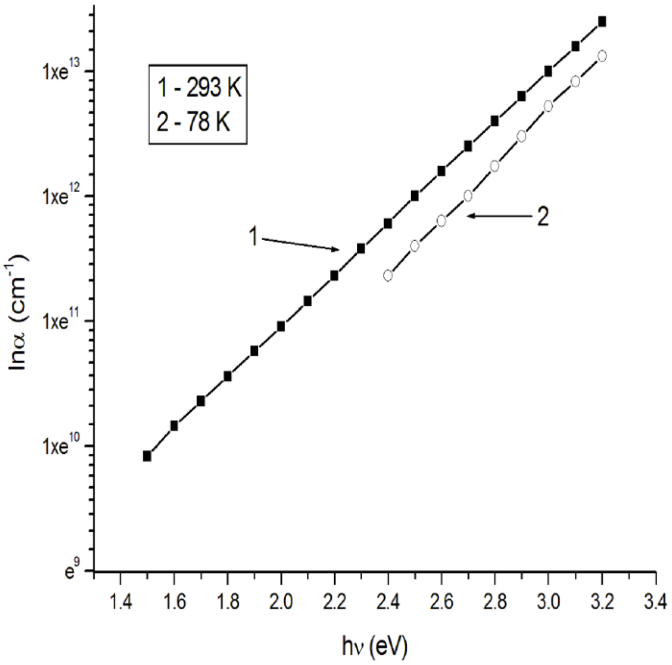

Fig. 3. The dependence of absorption coefficient on the photon energy, lnα=f(hν), in lower energy domain (Urbach rule).

The shift of the absorption edge to longer wavelengths implies that, qualitatively, the optical bangap energy E_g must shift to smaller value as degree of crystallinity increases. The E_g values depend on the type of model used for describing optical transitions across the gap. The values are in good agreement with the values reported for bulk ZnO crystals [1,27]. The determination of the energy bandgap from optical absorption seems to be more appropriate [6,29,31].

The studied ZnO thin films have a high transmission coefficient in visible spectral range (300 nm - 1600 nm).

It was established that the increase of the oxidation time determines an important decrease of the transmission coefficient. This behavior can be explained supposing a deterioration of a crystalline structure during oxidation process.

In the majority of investigations on the optical properties of polycrystalline semiconducting films, the effects of crystallite boundaries are neglected. Generally, the influence of crystallite boundaries on the optical properties is small [6,27].

The domain of lower energy range ($h\nu<E_{g,}$ where E_g is energy bandgap) absorption band at temperature 293 K and 78 K is well described by the exponential law (Urbach rule) [40-42]:

$$\alpha = \alpha_0 \exp\left[-\frac{\sigma_0\left(h\nu - h\nu_0\right)}{kT}\right] \tag{7}$$

where α_0 is the Urbach absorption at the edge $h\nu_0$, k is the Boltzmann constant, $kT/\sigma_0=E_u$ is the Urbach energy width, which depends on the structural disorder, hν is photon energy of incident radiation (hν=1.5 eV - 3.0 eV). [40-42]

Equation (7) is identic with following empiric expression [40,42,44]:

$$\alpha(h\nu) = \alpha_0 \exp\left[\left(h\nu - E_g\right)/E_u\right] \tag{8}$$

where E_g is the energy bandgap and α_0 and E_u denote the Urbach parameters.

As it was proved in [43], the dependence like (7) take place when the edge of absorption band is formed by the free excitons which interact with optical phonons [40-42].

The exponential dependence of the absorption coefficient on the incident photon energy, hν, in the "Urbach range" ($h\nu<E_g$) is due to the perturbation of the parabolic density of the states at the band edge and determines an increase of structural disorder (which, in his turn, determines an increase of E_u) [42,44].

Urbach expression is verified for a very large number of semiconductor crystals, in the low energy tail of the fundamental absorption band and also in impurity absorption bands, the absorption coefficient is well described by the exponential law (7) [40-43].

In polycrystalline films, the structural disorder is also determined to crystallite boundaries [6,39]

According to Eqs. (7) and (8), the dependences $\ln\alpha=f(h\nu)$ are linear . Consequently, by plotting lnα versus hν and fitting a straight line the values of parameters σ_0 and E_u can be determined [40,42,44]. Urbach energy can be calculated. Fig. 3 shows the dependences $\ln\alpha=f(h\nu)$ for a studied sample at two temperatures (78 K and 293 K).

For studied sample $\sigma_0=3.20\times10^{-3}$ at 293 K and $\sigma_0= 15.5\times10^{-3}$ at 78 K and $E_u=4.86$ eV at 293 K and $E_u=0.434$ eV at 78 K. The obtained values show that width of the band tail is greater at low temperature. σ_0 is called the steepness parameter which characterizes the absorption edge form determined by electron-phonon or/and exciton-phonon interactions.

3.2.2 Photoluminescence spectra

The study on the photoluminescence (PL) of ZnO thin films was used in order to evaluate the optical quality of respective films.

The following preparation conditions were used for oxidation of Zn metallic films: oxidation temperature, $T_{ox}=700$ K, oxidation time, $t_{ox}=90$ min. The zinc films were deposited onto SiO_2 substrates at room temperature. The film thickness was d=270 nm.

In Fig.4 the typical photoluminescence spectra are illustrated for two temperatures, $T_1=293$ K and $T_2= 78$ K.

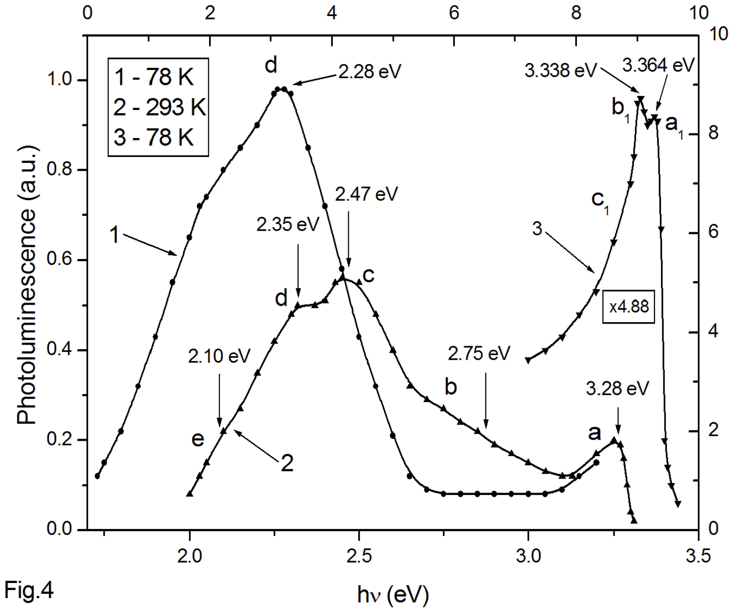

Fig. 4. Typical photoluminescence (PL) spectra for a ZnO thin film (sample ZNO.027.R, d=270 nm).

After oxidation, the films were submitted to a heat treatment within a temperature range ΔT=300-550 K.

It can be observed from Fig.4, that PL spectra revealed a complicated structure.

At temperature of 293 K, the spectral dependences of photoluminescence (Fig. 4, curve 2) is dominated by the edge band with a clear maximum at 3.28 eV (a) and a complex band with four sub-bands having an absolute broad maximum at 2.47 eV (c).

This emission bands at 2.47 eV are determined to the energy level of oxygen vacancies in the energy bandgap [45].

Several recent studies [46] have found that PL spectra of as doped ZnO:Ag film consist of one band with the emission maximum at 2.48 eV (800 nm). The emission is characterized by green colour.

We found that in visible spectral range, the photoluminescence consists of four sub-bands (indicated by a, b, c and d in Fig.4): two sub-bands are located in green-blue range of spectrum at 2.47 eV (c) and 2.35 eV (d), one sub-band in blue range with a weak maximum at 2.75 eV and another sub-band in the orange range of spectrum which has a maximum at 2.10 eV.

The (a) band as can be observed by comparison with the absorption spectra (Fig. 2) and photoluminescence spectra (Fig. 4) is shifted to smaller energies by 60 meV. This value is in a good agreement with Zn-O phonon in studied sample. It can be supposed that (a) band of photoluminescence is obtained as the radiant emission of excitonic transitions with the phonon emission with energy about 60 meV [31A].

The dominant band of PL spectra with peak position at 2.47 eV is determined by the recombination of hole from valence band with electron from singly-ionized level of oxygen vacancies [47].

The (b) band is considered as the luminescent recombination of an electron with small-energy-donor-level with a hole from valence band [20,27,42,44]. While the band (e) in the orange range is the result of recombination of non-equilibrium electrons from conduction band through ionized oxygen vacancies.

At the temperature of 78 K (Fig. 4, curves 1 and 3) the structure of two bands is kept in PL spectra. The dominant band from yellow range of spectrum has an impurity nature with the maximum at 2.280 eV (d). Also, at this temperature, the recombination band of electrons from the conduction band with bi-ionized oxygen vacancies (hν=2.10 eV) is present. The edge band at temperature T=78 K is decomposed into two sub-bands with maxima peaked at 3.338 eV (b_1) with an associated smaller peak centered at 3.364 eV (a_1) and a shoulder at 3.280 eV (c_1). The PL band with maximum at 3.338 eV is the result of annihilation of free excitons with the emission of optical phonons because the phonons energy in ZnO films is equal to about 70 meV.

As it seen that at temperature of 78 K the PL spectrum is dominated by a strong near-band-edge peak which is positioned at 3.28 eV.

This main peak may be attributed to the free-to-bound excitonic emission as peak positions did not change with energy values of excitation source.

The temperature dependence of the intensity of band with the maximum at 3.364 eV (a_1) was analyzed to establish the nature of this band. The temperature dependence of intensity in the temperature range from 140 K to 250 K can be described by the expression [47-49]:

$$I = I_0\left[1 + C\exp\left(-E/kT\right)\right]^{-1} \tag{9}$$

where *E* is the binding energy of charge carriers, *C* is the a parameter which doesn't depend on temperature, I_0 denotes the intensity of photoluminescence at 0 K.

The equation (9) can be written as

$$\frac{I_0}{I} - 1 = C\exp(-E/kT) \tag{10}$$

If we perform the logarithm, Eq. (9) becomes form:

$$\ln\left(\frac{I_0}{I} - 1\right) = \ln C - \frac{E}{k}\cdot\frac{1}{T} \tag{11}$$

As shown in Fig.5, the dependence $\ln(I/I_0\text{-}1)=f(10^3/T)$ is linear. The band energy E can be determined from the slope of the linear portions of these dependences and C parameter has been calculated by extrapolating these straight lines to $10^3/T \rightarrow 0$. The obtained values of E (E=65 meV) are in good agreement with those determined from the absorption spectra.

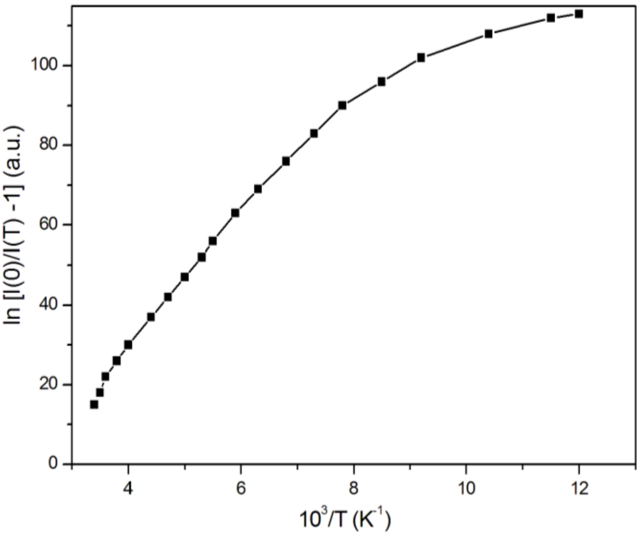

Fig. 5. The temperature dependence of the PL band intensity (sample ZNO.027.R, d=270 nm).

The PL is dominated by the emission at 3.338 eV. If the temperature increases the intensity of the main peak decreases indicating some optically active defects in studied samples [29,31,42].

The thermal activation energy of PL in this temperatures range is equal to 65 meV and it is the same as the exciton Ridberg (the binding energy of excitons) from absorption spectra. Therefore it can be concluded that the edge PL band is obtained as the annihilation of excitons which are bounded to ionized centers, probably oxygen vacancies.

4. Conclusions

Zinc oxide thin films were prepared by thermal oxidation of vacuum evaporated zinc metallic films onto glass substrates at room temperature (T=293 K) during film deposition.

The structural investigations show that the phase composition of ZnO films is not influenced by film thickness and used oxidation conditions.

The intrinsic absorption band of ZnO films is due to free excitons. The width of band gap at the temperature of 78 K of ZnO films is 3.459 eV.

The ZnO films have the intense photoluminescence in the UV and visible range of spectrum.

References

[1] H.L. Hartnagel, A.L. Dawar, A.K. Jain, C. Jagadish, Semiconducting Transparent Thin Films, Institute of Physics Publishing, Bristol and Philadelphia PA 1995.

[2] J.B. Lee, D.H. Cho, D.Y. Kim, C.K. Park, J.S. Park, Thin Solid Films, **516**, 475 (2007).

[3] N. Tsuda, K. Nasu, A. Fujimori, K. Siratori, Electronic Conduction in Oxides, Springer, Berlin-Heidelberg, 2000.

[4] A. El Amrani, F. Hijazi, B. Lucas, J. Boucle, M. Aldissi, Thin Solid Films, **518**, 4582 (2010).

[5] A.P. Râmbu, G.I. Rusu, Superlattices Microstruct., **47**, 300 (2010).

[6] L.L. Kazmerski (Ed.), Polycrystalline and Amorphous Thin Films and Devices, Academic Press, New York 1980.

[7] J.F. Chang, H.H. Kuo, I.C. Leu, M.H. Hon, Sensor Actuat B Chem **B4**, 258 (2002).

[8] S.R. Forrest, Appl. Phys. Lett. **84**, 3013 (2004).

[9] C.Y. Lee, Y.Y. Hui, W.F. Su, C.F. Liu, Appl. Phys. Lett., **92**, 261107 (2008).

[10] D.M. Bagnall, Y.F. Chen, Z. Zhu, T. Yao, S. Koyama, M.Y. Shen, T. Goto, Appl. Phys. Lett., **70**, 2230 (1997).

[11] S.A. Studenikin, M. Golego, M. Cocivera, J. Appl. Phys., **84**, 2287 (1998).

[12] M. Suchea, S. Christoulakis, N. Katsarakis, T. Kitsopoulas, G. Kiriakidis, Thin Solid Films, **515**, 6562 (2007).

[13] G.G. Rusu, M. Gârtan, M. Rusu, Superlattices Microstruct. **42**, 116 (2007).

[14] A.P. Râmbu, D. Sîrbu, G.I. Rusu, J. Vac. Sci. Technol. **A28**, 1344 (2010).

[15] E. G. Fu, D.M. Zhuang, W.F. Yong, M. Zhoa, Appl. Surf. Sci., **217**, 88 (2003).

[16] J.L van Heerden, R. Swanepoel, Thin Solid Films, **299**, 72 (1997).

[17] K.L. Chopra, S.R. Das, Thin Film Solar Cells, Plenum Press, New York, 1983.

[18] A. Abdallah, N. Tabet, M. Pastageer, S. Said, Phys. Status Solidi C, **8**, 1377 (2011).

[19] S. Ilican, Y. Caglar, M. Caglar, J. Optoelectron Adv. Mater. **10**(2), 2578 (2008).

[20] I.G. Wang, S. Plau, H.W. Lee, S.F. Yu, B.K. Tay, X.H. Zhang, H.H. Hug, J. Appl. Phys., **94**, 354 (2003).

[21] D. Sîrbu, A.P. Râmbu, G.I. Rusu, Materials Sci. Engin. B, **176**, 266 (2011).

[22] D.I. Rusu, G.G. Rusu, D. Luca, Acta Phys. Polonica A, **119**(6), 850 (2011).

[23] A. Ruijin, Lin Hong, Ling Xu, Herui Wen, Jinglin Chen, Jimsheng Liao, Weixiong You, Optical Materials, **345**, 786 (2012).

[24] G.G. Rusu, A.P. Râmbu, V.E. Buta, M. Drobromir, D. Luca, M. Rusu, Mater. Chem. Phys. **123**, 314 (2010).

[25] K. Bouzid, A. Djellonb, N. Bouzid, J. Bougdira, Phys. Stat. Sol. A, **206**(1), 106 (2009).
[26] K. Vanhensden, W.L. Warren, C.H. Seager, D.R. Tallant, J.A. Voigt, B.E. Gnade, J. Appl. Phys., **79**, 7983 (1996).
[27] C. Jagadiste, S.Y. Pearson (Eds), Zinc Oxide Bulk, Thin Films Nanostructure Processing, Properties and Applications, Elsevier, Amsterdam, 2006.
[28] G.G. Rusu, A.P. Râmbu, M. Rusu, J. Optoelectron Adv. Mater **10**(2), 339 (2008),.
[29] Y.N. Pankove, Optical Processes in Semiconductors, Dover, New York, 1971.
[30] K.L. Chopra, Thin Film Phenomena, McGraw-Hill, New York 1969.
[31] T.S. Moss, G. Burell, G.T. Elias, Semiconductor Optoelectronics, Wiley, New York, 1973.
[32] V. Chiricenco, M. Caraman, I.I. Rusu, C. Leontie, J. Lumin., **101**, 71 (2003).
[33] I.I. Uhanov, Optical Properties of Semiconductors, Science, Moscow, 1977 (in Russian).
[34] Joint Committee Power Diffraction Standards, Power Diffraction File (Data file no. 36-1451-ZnO).
[35] B.D. Cullity, S.R. Stock, Elements of X-Ray Diffraction, Prentice Hall, 2001, 3rd ed.
[36] H. Metin, R. Esen, Semicond. Sci. Technol., **18**, 647 (2003),.
[37] C.S. Barret, F.B. Massalski, Structure of Metals, Pergamon Press, Oxford, 1980.
[38] J. Tauc, A. Menthe, J. Non-Cryst, **569**, 8 (1972).
[39] G.I. Rusu, M.E. Popa, G.G. Rusu, I. Salaoru, Appl. Surf. Sci., **218**, 222 (2003).
[40] F. Urbach, Phys. Rev., **92**, 1324 (1953).
[41] T.H. Keil, Phys. Rev., **149**, 582 (1966).
[42] N.F. Mott, E.A. Devis, Electron Processes in Non-Crystalline Materials, Clarendon Press, Oxford, 1972.
[43] Y. Liu, L. Zhao, J. Lian, Vacuum **81**, 18 (2006).
[44] L. Bentes, R. Ayouchi, C. Santos, R. Schwarz, P. Sanguino, O. Conde, M. Peres, T. Monteiro, O. Teodoro, Superlattices Microstruct., **42**, 152 (2007).
[45] Hao-Ying Lu, Sheng-Yuan Chu, Soon-Seng Tan, J. Cryst. Growth, **269**, 385 (2004).
[46] V.S. Khomchenko, T.G. Kryshtab, A.K. Savin, L.V. Zavyalova, N.N. Roshchina, V.E. Rodionov, O.S. Lytvyn, V.I. Kushnirenko, V.B. Khachatryan, J.A. Andraca-Adame, Superlattices Microstruct., **42**, 94 (2007).
[47] Y.G. Wang, S.P. Lau, X.H. Zhang et al, Chem. Phys. Lett., **375**, 113 (2003).
[48] S. Seto, A. Tanaka, Y. Masa, M. Kawashima, J. Cryst. Growth, **117**, 271 (1992).
[49] R.E. Dietz, J.J. Hopfield, D.G. Thomas, J. Appl. Phys., **32**, 2282 (1961),.